AFML-TR-75-138

A STUDY OF THE UNSTEADY FLOW OVER CONCAVE CONIC MODELS AT MACH 15 AND 20

VON KARMAN INSTITUTE FOR FLUID DYNAMICS
CHAUSSEE DE WATERLOO, 72
1640 RHODE-ST-GENESE, BELGIUM.

OCTOBER 1975

TECHNICAL REPORT AFML-TR-75-138
INTERIM SCIENTIFIC REPORT NO.2
1 JUNE 1972 – 30 NOVEMBER 1973

AIR FORCE MATERIALS LABORATORY
AIR FORCE WRIGHT AERONAUTICAL LABORATORIES
Air Force Systems Command
Wright-Patterson Air Force Base, Ohio 45433

NOTICE

When Government drawings, specifications, or other data are used for any purpose other than in connection with a definitely related Government procurement operation, the United States Government thereby incurs no responsibility nor any obligation whatsoever; and the fact that the government may have formulated, furnished, or in any way supplied the said drawings, specifications, or other data, is not to be regarded by implication or otherwise as in any manner licensing the holders or any other person or corporation, or conveying any rights or permission to manufacture, use, or sell any patented invention that may in any way be related thereto.

This final report was submitted by the von Karman Institute, 72, Chaussee de Waterloo, 1640 Rhode-St-Genèse, Belgium, under contract AFOSR-72-2227, with the Air Force Materials Laboratory, Air Force Wright Aeronautical Laboratories, Air Force Systems Command, Wright-Patterson Air Force Base, Ohio, 45433. George Y. Jumper, Jr., Capt., USAF, with the Space and Missiles Branch, Systems Support Division was the Project Engineer.

This report has been reviewed by the Information Office (IO) and is releasable to the National Technical Information Service (NTIS). At NTIS, it will be available to the general public, including foreign nations.

This technical report has been reviewed and is approved for publication.

Everett W. Heinonen

EVERETT W. HEINONEN, Capt, USAF
Project Engineer

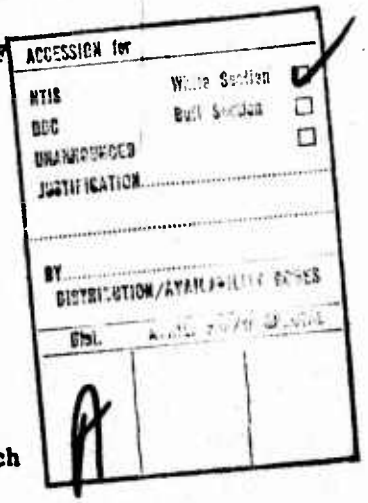

FOR THE DIRECTOR

Henry E. Beck

HENRY E. BECK, Major, USAF
Chief, Space and Missiles Branch
Systems Support Division
AF Materials Laboratory

Copies of this report should not be returned unless return is required by security consideration, contractual obligations, or notice on a specific document.

AIR FORCE - 9-1-76 - 100

Unclassified

SECURITY CLASSIFICATION OF THIS PAGE (When Data Entered)

(19) REPORT DOCUMENTATION PAGE

READ INSTRUCTIONS BEFORE COMPLETING FORM

(18) 1. REPORT NUMBER: AFML-TR-75-138

2. GOVT ACCESSION NO.

(9) 3. RECIPIENT'S CATALOG NUMBER

(6) 4. TITLE (and Subtitle): A STUDY OF THE UNSTEADY FLOW OVER CONCAVE CONIC MODELS AT MACH 15 AND 20.

5. TYPE OF REPORT & PERIOD COVERED: Interim Scientific Rept. 1 Jun 72 — 30 Nov 73.

6. PERFORMING ORG. REPORT NUMBER

(10) 7. AUTHOR(s): M.A. KENWORTHY and B.E. RICHARDS

(15) 8. CONTRACT OR GRANT NUMBER(s): VAF AFOSR-2227-72

9. PERFORMING ORGANIZATION NAME AND ADDRESS: von Karman Institute for Fluid Dynamics, 72, Chaussée de Waterloo, 1640 Rhode-St-Genèse, Belgium

10. PROGRAM ELEMENT, PROJECT, TASK AREA & WORK UNIT NUMBERS: 62102F (17) 738102 (16) AF-7381-02

11. CONTROLLING OFFICE NAME AND ADDRESS: EOARD (Box 14, FPO N.Y. 09510) (12) 56 p.

12. REPORT DATE: Sep 75 (11)

13. NUMBER OF PAGES: 48

14. MONITORING AGENCY NAME & ADDRESS (if different from Controlling Office): EOARD (Box 14), FPO N.Y. 09510

15. SECURITY CLASS. (of this report): Unclassified

15a. DECLASSIFICATION/DOWNGRADING SCHEDULE

16. DISTRIBUTION STATEMENT (of this Report)

Approved for public release; distribution unlimited

17. DISTRIBUTION STATEMENT (of the abstract entered in Block 20, if different from Report)

Approved for public release; distribution unlimited

18. SUPPLEMENTARY NOTES

19. KEY WORDS (Continue on reverse side if necessary and identify by block number)

Hypersonic Flow
Re-entry
Ablation
Nose Shapes
Unsteady Flow
Pressure Measurements
High Speed Photography

20. ABSTRACT (Continue on reverse side if necessary and identify by block number)

Pressure measurements and high speed cone schlieren photography have been used to study the unsteady flow behaviour of the Mach 15 and 20 flow over families of concave conic model shapes. The test flow parameters achieved closely simulate aerodynamic re-entry conditions. The unsteady flow behaviour was found to resemble that found on certain configurations of spike cones. The shape of the concave surface and the Reynolds number were found

DD FORM 1 JAN 73 1473A EDITION OF 1 NOV 65 IS OBSOLETE

Unclassified

SECURITY CLASSIFICATION OF THIS PAGE (When Data Entered)

to 14738

367 475

from 1473A

to be important parameters controlling the type of unstability. Further test programmes are considered necessary to understand the flow processes and to define the boundaries of the instabilities.

1473B

PREFACE

The activities and results documented in this report were supported under project 7381 "Materials Application", Task 7381-02 "Space, Missile and Propulsion System Materials and Component Evaluation" with Mr. Gary L. Denman, Technical Manager for Thermal Protective Systems, System Support Division, Air Force Materials Laboratory, acting as project engineer. The report covers work conducted during the period June 1972 through December 1973.

The technical advice and guidance by Mr. Victor Di Cristina, Manager, Thermodynamics and Material Test Department, Avco Systems Division, Avco Corporation, Wilmington, Mass., Dr. Michael Abbett, Accurex/Aerotherm, Moutain-View, California, and their colleagues was particularly valuable. The authors acknowledge the help given by Mr. Roger Conniasselle and members of the Longshot personnel, members of the electronics department, and Mr. Jean-Paul Lobet and his assistants of the photographic laboratory.

TABLE OF CONTENTS

LIST OF FIGURES

LIST OF TABLES

SECTION I

INTRODUCTION

The problem of predicting the behaviour of ablative thermal protection components on re-entry vehicles is very complex. In addition to the problem of understanding the interaction between chemical and aerodynamic processes inherent on any ablative surface, there has arisen evidence that flow instabilities occur on a certain family of ablation shapes (i.e. those with concave conical forebodies).

These particular shapes are formed during the high Reynolds number portion of re-entry when the boundary layer on the forebody is turbulent. Then the peak heat transfer and hence, peak mass transfer rate takes place away from the stagnation point. The shape which is thus generated from an initially hemispherical forebody has this concave form which resembles the spiked blunt body of classic gasdynamics (Figure 1).

The purpose of the present investigation was to measure, at realistic re-entry Mach and Reynolds numbers, frequencies and pressure levels of fluctuating phenomena on two specific concave geometries. One model was the AVCO Concave Biconic Model used in an earlier study (Reference 1) for primarily heat transfer measurements, when the flow was then tentatively classified as stable. The model was re-instrumented with BBN fast response pressure sensors to look more closely for the possible existence of the less violent flow instabilities.

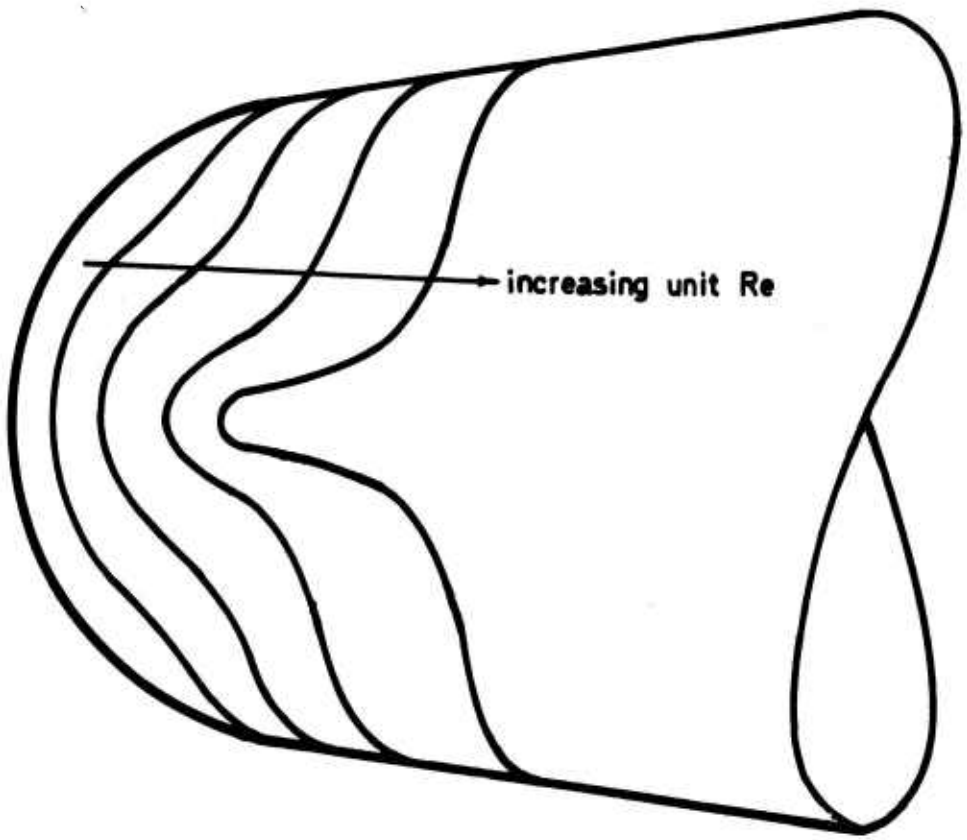

Figure 1 History of a Typical Re-entry Ablation Nose

The other model was Aerotherm's Triconic Model which was instrumented with fast response Kulite pressure transducers.

Before presenting the results of this study a review of investigations made into flow instabilities over spiked cones is made. This is considered useful since a large body of research exists on spiked bodies, due to the early interest in their apparent ability to alleviate high total heating rates and reduce the drag of high speed vehicles (e.g. Allen and Eggers, Reference 2 and Moeckel, Reference 3).

SECTION II

BRIEF REVIEW OF RESEARCH ON INSTABILITIES ON SPIKED BLUNT BODIES

1. INTRODUCTION

Early in the research on spiked blunt boides flow instabilities were observed. Mair (Reference 4), Beastall and Turner (Reference 5), Bogdonoff and Vas (Reference 6), Maull (Reference 7), Wood (Reference 8) and Holden (Reference 9) showed that for a given Mach number, M, cone half angle θ_c, and shoulder radius r, there exists a range of values of the ratio of spike length 1, to body diameter, D, such that the flow is unstable (as illustrated in Figure 2). For example, at M=6.8 for a flat-faced (θ_c=90°) square shouldered body (r=0) it was found by Maull (Reference 7) that the flow was unstable for $0.25 \leq 1/D \leq 2.5$.

2. DESCRIPTION OF MODELS OF INSTABILITY

There have been observed basically three modes of instability as illustrated in Figure 3. The manifestation of the first is a dramatic excursion between two very different shock envelopes. The first envelope consists of a conical oblique shock emanating from the spike tip intersecting a bow shock created by the blunt body. The second consists of a shock passing through the spike tip as though mass was being blown from the face of the blunt body. In fact, Maull (Reference 7) obtained this latter shock pattern by simply injecting gas through a tube pointing into a hypersonic free-stream. This mode of instability is known as pulsation and occurs at the lower end of the unstable range of 1/D depending

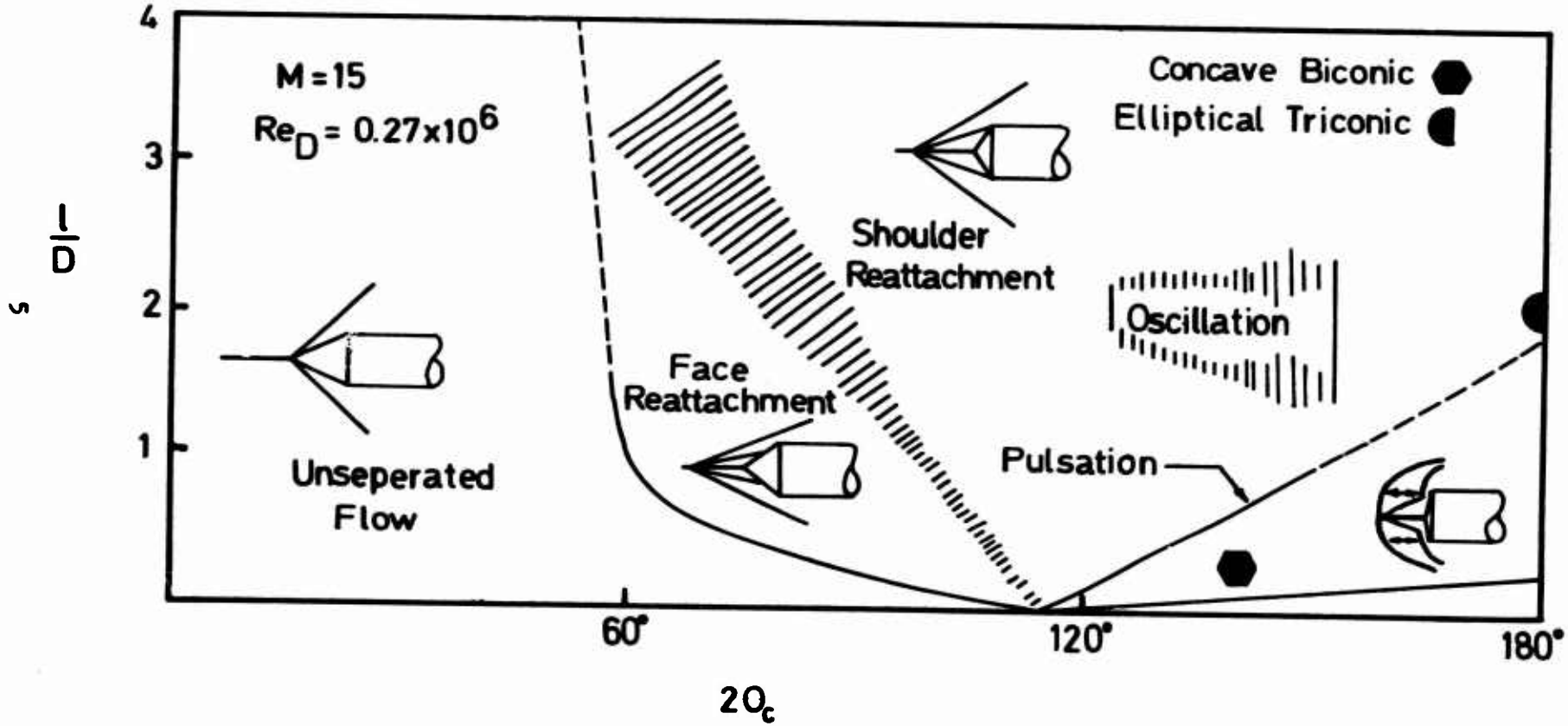

Figure 2. Flow Regions for Spiked Cones after Holden (Ref. 9)

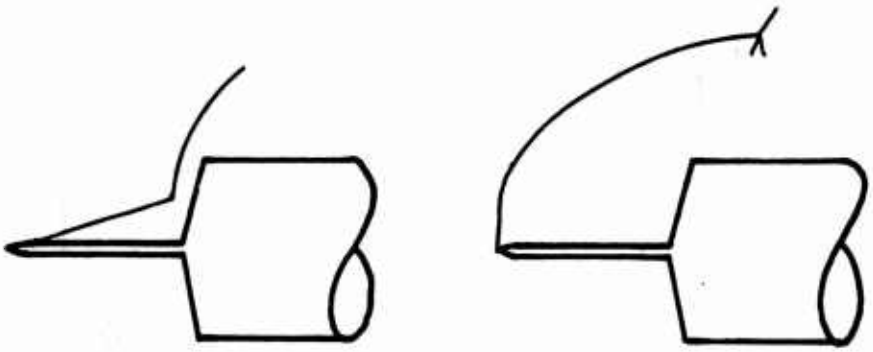

Pulsation

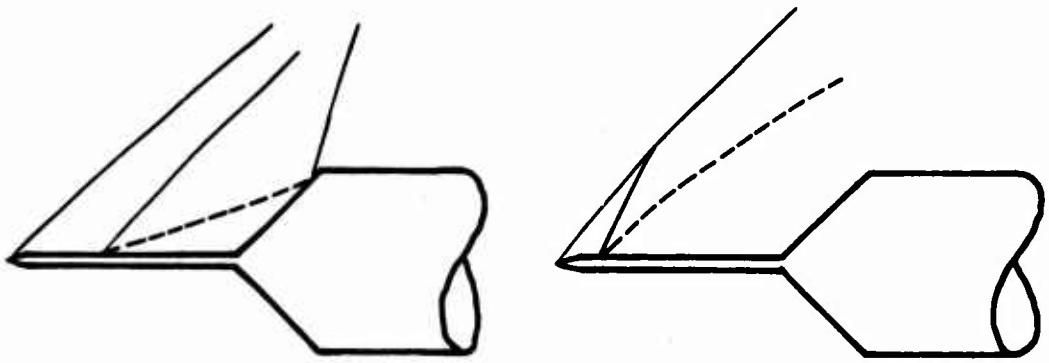

Oscillation

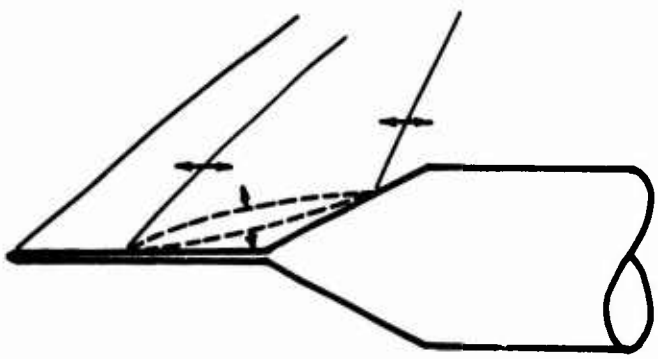

Vibration

Figure 3. The Three Modes of Flow Instability

on free stream conditions. The other two modes are less dramatic in that the two shock systems remain in evidence at all times.

The second mode, as illustrated in Figure 3 and called "oscillation", involves both changes in the inflection of the conical shock and in the volume of the conical shock region.

The third mode called "vibration", not seen by all investigators (see Kabelitz, Reference 9), involves just a change in inflection of the dividing streamline and small vibrations of the shock waves.

Both of these latter models of instability occur at the larger values of l/D.

The occurrence of these two particular modes depends apparently on the cone half angle ; the smaller cone half angles causing vibration and larger cone half angles causing oscillation.

3. FLOW MODELS USED

Some flow models for one or all of the modes of instability have been suggested by various researchers. For example Maull (Reference 7) describes the instability with a model involving mass addition to the originally conical separated flow region due to an imbalance of pressures behind the intersection of the conical foreshock and the near-normal aftershock. As the separated region broadens, pressure equilibrium is obtained and the separation-bubble collapses.

Another model suggested by Kabelitz (Reference 10) involves the response of the closed separated region to perturbations. That is, small fluctuations in the freestream amplify themselves for certain geometrical and flow configurations. Another is the piston model which considers an approximately normal shock moving toward the blunt body compressing the air. Finally this high density air strikes the body creating a reflection which in turn merges with the original normal shock causing a rapid expansion or explosion. This expansion continues until equilibrium is reached with the freestream and then collapses to begin the compression cycle again (Reference 11).

4. DISCUSSION

Despite the relatively large amount of data that exists to date on flow instabilities on spiked blunt bodies, many uncertainties still exist. These concern mainly the definition of the mechanism of the flow instability and the prediction of the conditions under which they occur. It is clear that there is a very strong interaction between the inviscid and viscous flows involved. Parameters of interest in applying experience of flows over spiked blunt bodies to those over concave conic shapes associated with re-entry shapes include Mach number, Reynolds number, l/D, nose bluntness, shoulder radius, spike-to-body fairing, wall temperature, surface roughness, etc. These parameters will furthermore affect the nature of the viscous flow (e.g. concerning whether laminar, transitional or turbulent flow is present; concerning the resistance of the boundary layer to separation, etc.). Also the flow will have mixed subsonic and supersonic regions. As will be seen insection 4 of this report, the results from concave conic sections are extremely difficult

to analyse with such uncertainties present. An indication of the errors that may be incurred in applying spiked blunt body data to understanding flows over concave conic shapes is illustrated in the results of this present study. Section 4 describes how the flow over the Concave Biconic Model mostly appears stable (i.e. pulsation mode absent) while the Elliptic Triconic is mainly unstable (i.e. pulsation mode present). The shape of the models defined in terms of representative values of 1/D and $2\theta_c$ plotted in Figure 2 illustrate that the reverse behaviour would be expected. It is recommended then that a well planned series of experiments backed up by flow analysis calculations be carried out using the spiked cone configuration as a basis to provide a better understanding of the topic.

SECTION III

EXPERIMENTAL APPARATUS AND PROCEDURE

1. TEST FACILITY

The von Karman Institute Longshot test facility was used for this program, Longshot differs from a conventional gun tunnel in that a heavy piston is used to compress the nitrogen test gas to very high pressures and temperatures (reference 12). The test gas is then trapped in a reservoir at peak conditions by the closing of a system of check valves. The flow conditions decay monotonically during 10 to 20 milliseconds running times as the nitrogen trapped in the reservoir flows through the 6° half-angle conical nozzle into the pre-evacuated open jet test chamber. The maximum supply conditions used in these tests are approximately 4000 atmospheres at 2000°K to 2400°K. These provide unit Reynolds numbers of 8.5×10^6 and 2×10^6 per ft. at nominal Mach numbers of 15 and 20. The two Mach numbers were obtained at the 14 in. diameter nozzle exit plane by using throat inserts with different diameters.

2. MODELS

a. Concave Biconic Model

The Concave Biconic Model supplied by AVCO Systems Division, consisted of a convex forebody which is smoothly faired into 14° half-angle conical after body which has a base diameter of 6.25 in. (see Figure 4).

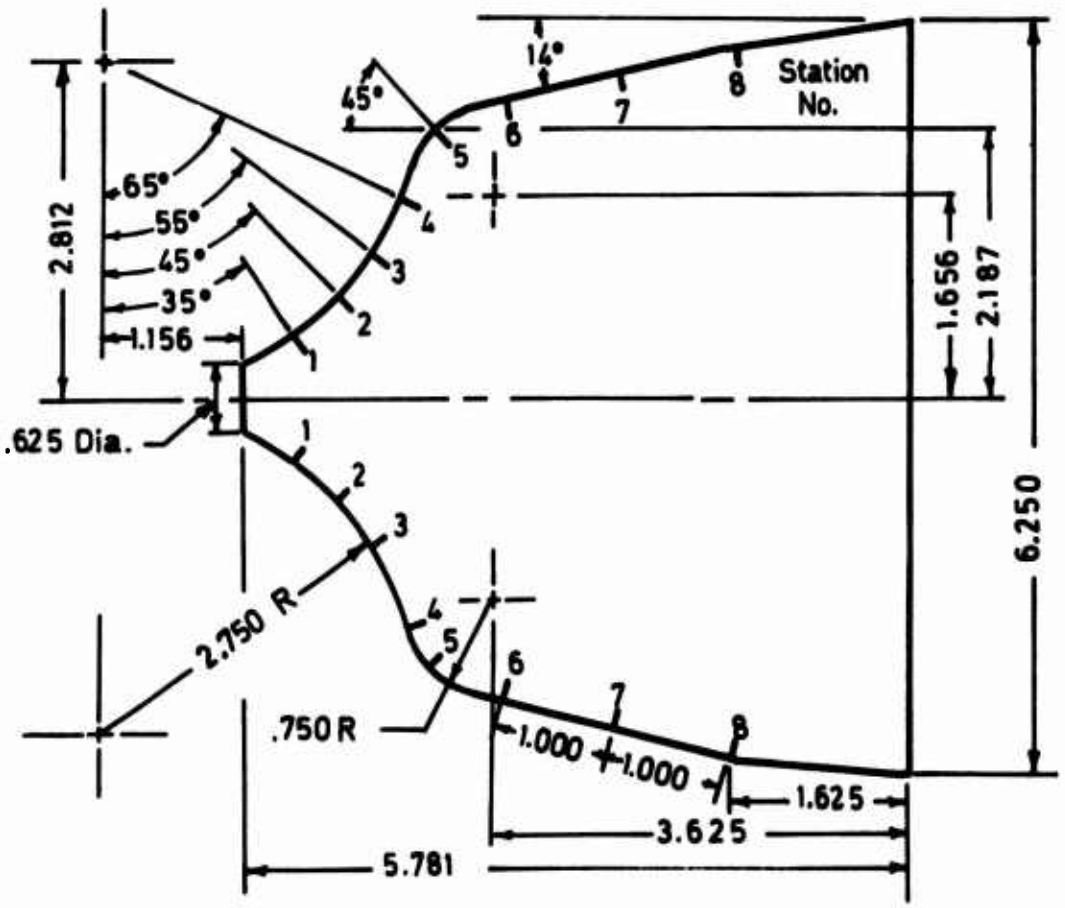

Configuration of the Basic Body

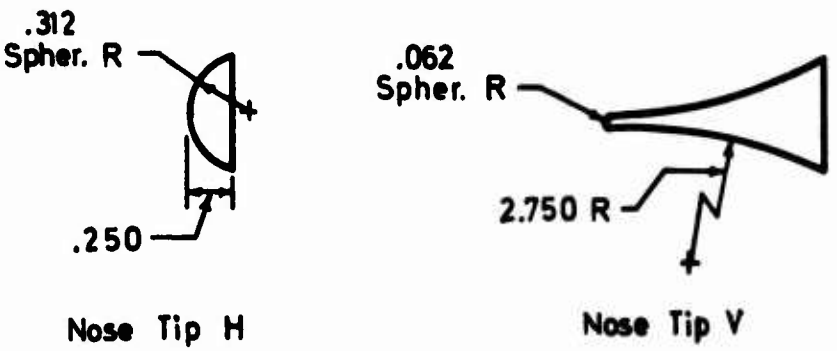

Nose Tip H

Nose Tip V

Figure 4. AVCO Concave Biconic Models

The model radius at the forebody-afterbody junction (referred to later as the model shoulder) was 2.187 in. The radius of the generator defining the concave forebody was 2.75 in. giving a surface angle change from 24° to 70° to the model axis.

Two interchangable nose tips were used. One, supplied by AVCO, was a 0.312 inch hemisphere ; the other, manufactured at VKI, was simply a continuation of the circular concave section until the body surface angle was at zero incidence with the freestream and hemispherically capped. See figure 4. The first configuration was designated model H and referred to descriptively as the blunt biconic model. The second configuration was designated model V and also referred to as the sharp biconic model.

The model was equipped with 8 wall pressure taps located along a single meridian. However, only stations 2, 3, and 4 as illustrated in figure 1 were instrumented. Steady pressure measurements were made using a Hidyne pressure transducer at station 2 only. Unsteady pressure measurements were made using BBN type 377 piezoelectric pressure sensors at stations 3 and 4. Details for both types of instrumentation are given in Section III.3.b.

b. Elliptical Triconic Model

This model supplied by Aerotherm, was similar to the Concave Biconic Model except the concave portion of the forebody was generated by an ellipse with the major axis perpendicular to the model axis (see figure 5). The surface angle of the concave surface referenced to the model axis changed from 0° to 90°.

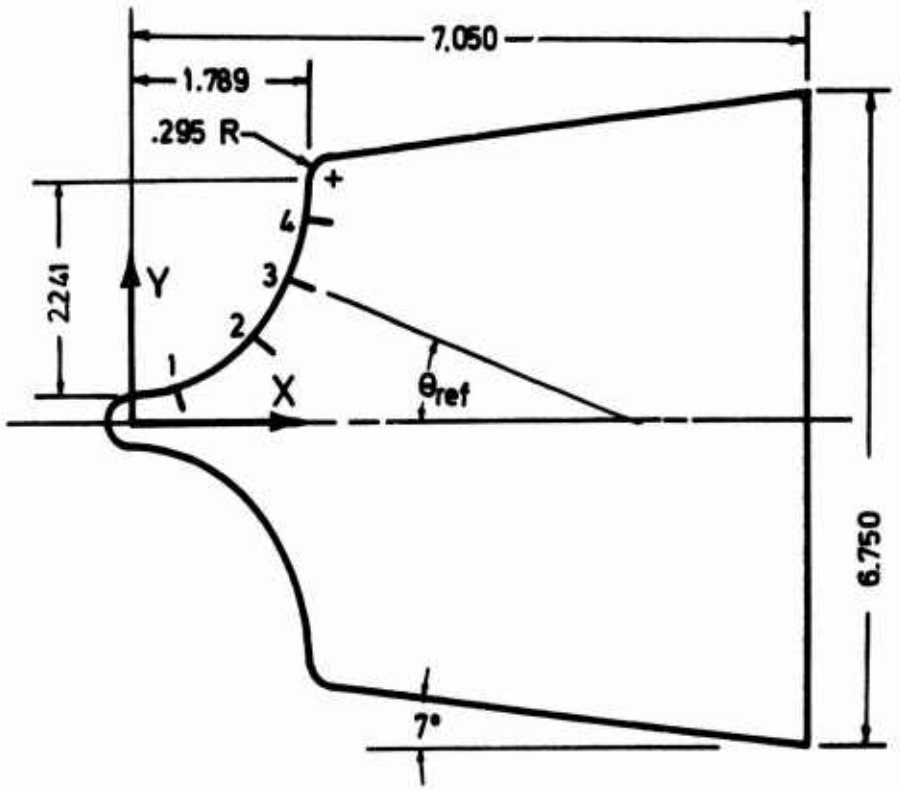

Station No.	1	2	3	4
X	.440	1.250	1.590	1.770
Y	.316	.878	1.459	2.168
θ_{ref}	73.5°	39.13°	22.15°	6.6°

Figure 5. Aerotherm Elliptical Triconic Model

This model was supplied with four interchangable nose tips. Two were hemispherically shaped with 0.25 in radii, one having a smooth surface and the other having a surface roughness of approximately 0.004 in average element height caused by a chem-etching process. The other two tips were similar except the hemispherical sections were placed at the end of 0.25 in radius cylindrical extensions of 0.50 in length.

Four pressure taps were placed axially along the elliptical section of the forebody. Details of the Kulite pressure sensors used are given in Section III.3.c.

3. PRESSURE INSTRUMENTATION

a. Hidyne variable reluctance gauges

Steady pressure measurements on the Concave Biconic models H and V were measured using Hidyne variable reluctance transducers. A description of them, their calibration and application is given in Reference 13.

b. BBN piezo-electric transducers type 377

For measuring the expected fluctating pressures on the Concave Biconic model surfaces, BBN type 377 piezo-electric pressure sensors with an internal impedance matching circuit (FET) were used. The total dimension of these sensors (including FET circuit) are 0.11 in diameter by 0.75 in long; the sensing diameter is 0.08 in. Their sensitivity is about 100 mV/psi over a frequency range from 50 Hz to beyond 200kHz; resonance frequency is above 250 kHz. The transducers were excited by BBN battery operated power supplies and the signals were recorded on Tektronix type 502 A oscilloscopes with a

Polaroid camera, or on a CEC type ultra-violet oscillograph using CEC type 7-361 galvanometers with frequency response up to 5 kHz. The dynamic calibration curves of these transducers was supplied by BBN. In three tests, two of these transducers were mounted flush with the surface of model H at stations 3 and 4 as defined in figure 4. The installed sensors were covered with an RTV layer, smoothed to the surface contours. This technique has been used in the past, showing no evidence of deterioration in sensor performance. These transducers have been used successfully before in the Longshot tunnel for measuring fluctuation pressures as described in Reference 14.

c. Kulite piezo-resistive gauges type XTEL-190-100

The transducers used for measuring fluctuating as well as steady pressures on the Elliptic Triconic Model were Kulite piezo-resistive gauges type XTEL-190-100. The pressure sensitive component of these transducers which have pressure ratings of 100 psi consisted of a fully active four arm Wheatstone bridge diffused on a silicon diaphragm and included temperature compensation. The dimensions of these sensors are 0.140 in diameter by 0.61 in length with a pressure sensing area of 0.085 in diameter. Their nominal sensitivity is 0.75 mV/psi using a d.c. excitation voltage of 5 volts, over a frequency range from 0 to approximately 100 kHz (their natural frequency being greater than 100 kHz).

The transducers were excited by battery operated 5 volts rating power supplies fabricated by VKI. The signals were amplified using d.c. amplifiers (again fabricated by VKI) with a flat frequency response beyond 100 kHz and recorded simultaneously in three different modes. The output from

the amplifier was recorded on Tectronix 502 A oscilloscopes in filtered and unfiltered modes. The R-C filters used had flat responses to 1 kHz, 3dB down at 7kHz and with a 9dB/octave attenuation cut off beyond 15 to 20 kHz. The filters were used to remove unwanted very high frequency signals caused by wind tunnel background noise and vibrations. The signals were also recorded on the CEC ultra-violet oscillograph recorder described earlier, which also caused the signals to be filtered at frequencies above 5 kHz.

Four of these transducers provided the sole instrumentation used on the Elliptical Triconic model as shown in igure 5. The Kulite gauges were mounted in a ported configuration (diameter of port 0.06 in., length of port 0.10 in.). Tests carried out by Aerotherm in a shock tube indicated that this was a suitable geometry for fluctuating pressure measurements in that oscillations were damped out twice as fast as in a flush-mounted configuration.

4. DYNAMIC CALIBRATION OF KULITE GAUGES

A dynamic calibrator has been fabricated at VKI, which can supply pressure steps of up to 2 atmospheres in a rise time of about 1 msec. The calibrator is similar to that described in Reference 15. The transducers were calibrated while installed in the model and connected to the instrumentation used in the tests. The pressure was applied to the pressure taps through an adaptor. Sealing was obtained by hand pressing the adapter fitted with an O-ring seal to the model surface. A flexible tube was used to connect the adaptor to the calibrator. The connecting passage had an approximate internal diameter of 0.06 in and an overall length

of 15 in. A typical calibration trace is seen in figure 6. The damped oscillation is caused by the "organ pipe" effect created by the use of a long tube. The result shows that the transducer responds to both the d-c and a-c modes of the applied pressure variation. All four transducers responded identically except regarding the overall sensitivity. The pressures calculated from the steady part of the trace were generally 4 % below that monitored. This was ascribed to difficulties in scaling caused by applying the adaptor to curved surfaces.

5. SCHLIEREN PHOTOGRAPHY

An 18 in. conventional single pass Toepler schlieren system equipped with high quality optical components is used. With the exception of one 24 in. diameter plane mirror to bend the light 90° (due to the vicinity of a wall near the test section) the light beam takes a Z-shaped path. A single spark light source with a spark duration of 1 μsec is used in one test to record the visualization of the flow on 3 1/4 x 4 1/4 in sheet film. In the remaining tests high speed ciné schlieren photographs were taken using 16 mm Kodak ciné camera. Framing rates of 10,000 per second were achieved during the running time by operating the camera without the rotating prism shutter and exposing the film to appropriately sequenced multiple sparks of approximately 1 μsec duration.

6. TEST MATRIX

The test conditions obtained were computed using the Longshot data reduction program as outlined in Reference 13. Measured reservoir conditions and Pitot pressure are given in

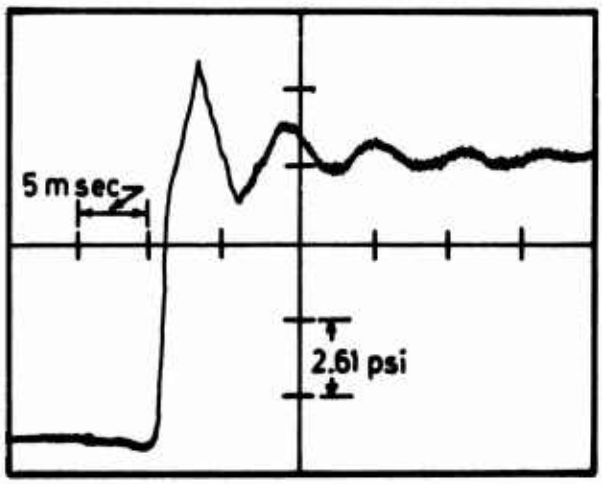

Δp input = 11 psi

Figure 6. Typical Dynamic Calibration Trace

Table 1 followed by the Mach and Reynolds numbers calculated in the section. Also noted is the model configuration.

The Concave Biconic Model was tested at generally the lower Reynolds numbers, i.e. Mach 20 with a unit Reynolds number of 3.1×10^6/ft and Mach 15 at 4.6×10^6/ft. The Elliptical Triconic Model was subjected to the latter flow for only one test with the remaining tests in the Mach 15 flow with a unit Reynolds number of 8.7×10^6/ft.

TABLE 1

TEST MATRIX

RUN	MODEL	NOSE	Po (psia)	To+ (°K)	PITOT (psia)	M++	Re/ft (X10-6)	SCHLIEREN
466	CBi†	H	59000+	2350	7.82	20.0	3.3	Spark
467	ETri†	Long Rough	55000+	1900	24.8	16.3	8.6	Ciné
468	ETri	Long Rough	34500	2020	13.8	15.7	4.5	Ciné
469	ETri	Long Smooth	60500	1900	22.7	17.0	8.7	Ciné
470	ETri	Short Rough	61000	1900	23.9	16.9	8.7	Ciné
471	CBi	H	36500	2020	14.9	15.7	4.8	Ciné
472	CBi	V	36500	2020	15.2	15.7	4.8	Ciné

+Assessed from previous runs

++Determined from (Po) equiv. perf. and measured P_{t2} in test section

†CBi - Concave Biconic

ETri - Elliptical Triconic

SECTION IV

RESULTS AND DISCUSSION

1. EXPERIMENTS USING THE AVCO CONCAVE BICONIC MODELS

a. Flow observations from Schlieren Photographs

The blunt nosed Concave Biconic Model, designated H in reference 1, was subjected to first the high Reynolds number, 3.1 x 10^6/ft, Mach 20 flow (designated Run 466) and then to the low Reynolds number, 4.6 x 10^6/ft, Mach 15 flow (Run 471). A simple spark schlieren of the first test and a high speed ciné schlieren of the second showed the flow to be stable in that there was no apparent movement of the shocks. See Figure 7 and Figure 8. The single spark visualisation technique for detecting instabilities was not considered definitive because it only allowed a single discrete sample of the flow to be made. However, Figure 7 reveals a bright luminous area just behind the after shock which is the result of tiny dust particles present in a high temperature region (3000°K) of shock heated gas. Because the shutter itself is open for 100 msec, any movement of the shock would have been recorded as a smear of this luminous area. The high speed ciné schlieren is a more definite form of proof that the shock envelope was stable.

b. Results of pressure measurements

The output signal from the high frequency BBN pressure sensors, however, did reveal fluctuations. During Run 466 only unfiltered traces were recorded which revealed very high frequencies (estimated at 50 - 100 kHz) with amplitudes of approximately one half the peak pitot pressure.

The amplitude, Δp, of these fluctuations did not decay with time, as do the absolute pressures, but remained approximately constant. During Run 471 all signals from the BBN pressure sensors were recorded in both filtered and unfiltered modes. The unfiltered signals were similar in frequency to those obtained in Run 466. The value of Δp was somewhat lower at 0.15 (P_{t2}) peak. The filtered trace at station 4, however, revealed that there also existed a very regular fluctuation of frequency approximately 7 kHz and a Δp of 0.07 p_{t2}.

c. Discussion of Tests on Concave Biconic Model H

Estimates of the frequency for the pulsation mode of instability calculated from correlations of the Strouhal number based on body diameter were around 3 kHz. Pallone (Reference 11) in testing a different model found a Δp of 1.5 p_{t2} for this mode at the lowest Reynolds number conditions in his experiments. It is therefore surmised that the high frequency (50 - 100 kHz) content of the output of the pressure sensors would most likely be due to a number of causes, e.g. pressure fluctuations associated with a turbulent boundary layer or a small locally separated region, background noise from the tunnel itself or possibly mechanical vibrations transmitted to the model through the sting mount. The very regular 7 kHz signal, however, demonstrates the possible existence of the vibrational mode of instability not seen in the earlier tests (Reference 1) in which only high speed schlieren pictures were taken since this mode involves no large displacement of the shock waves. Later in this report the pulsation mode was detected in tests on the Elliptic Triconic model whose surface at the shoulder forms a 90° angle with the freestream as compared to the 70° of the concave biconic. As stated earlier, the vibrational mode is associated with smaller cone angles hence it would appear plausible that the Concave Biconic model would more likely

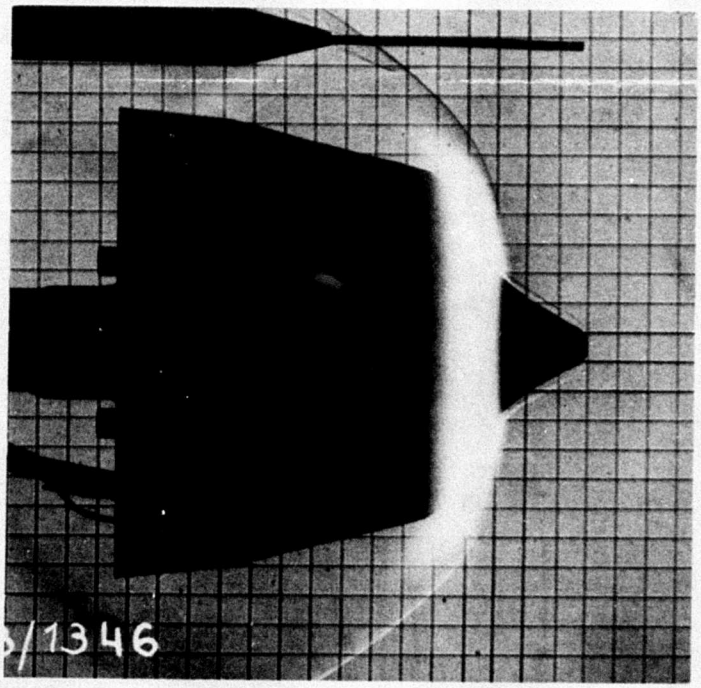

Figure 7. Spark Schlieren of Model H at M=20

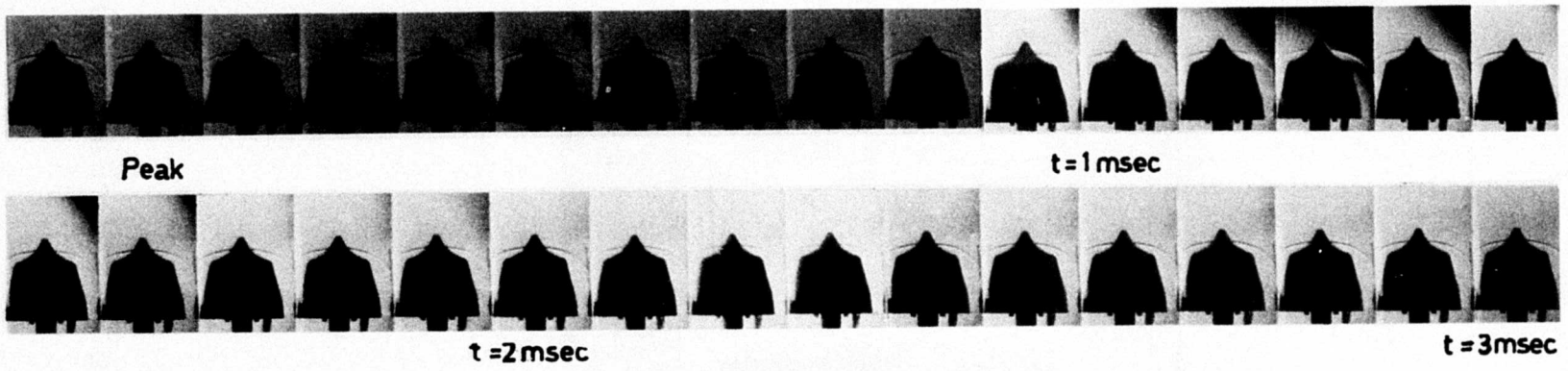

Model H (Run 471)

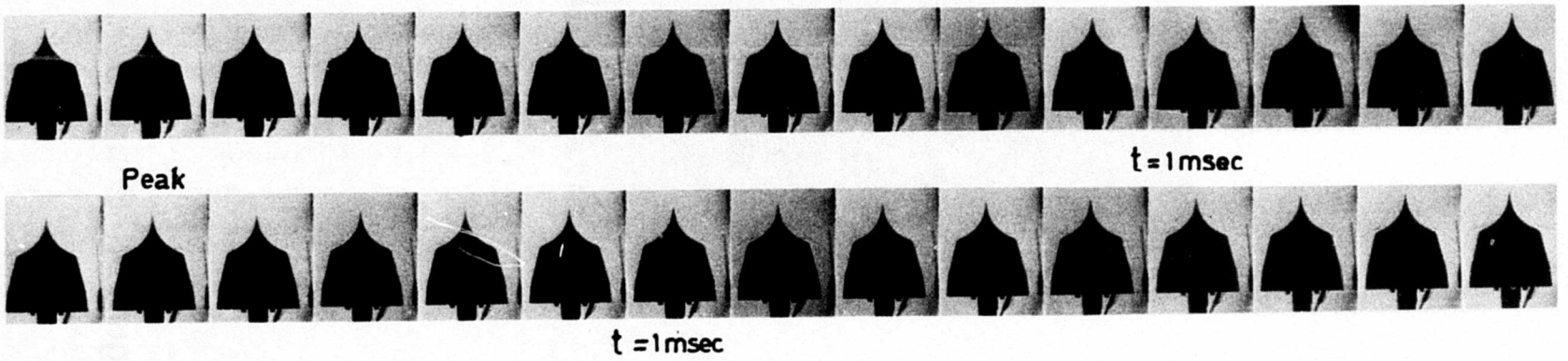

Model V (Run 472)

Figure 8. High Speed Ciné Schlieren of Models H and V at M = 15

support this particular mode.

d. Results and discussion of Tests on Concave Biconic Model V

The results of a third test employing the Concave Biconic Model V appeared very different from previous tests in that two types of flow behaviour were detected with both the pressure transducers and ciné photographs. For the first millisecond the flow resembled quite closely the flow patterns described in the preceding paragraphs in which the existence of "vibrational" instability was suggested. A foreshock emanated from the nose tip and developed very close to the body until it intersected the aftershock. The aftershock itself was very nearly normal at the point of intersection and appears as a bow wave associated with a blunt body. In fact, the shock stand-off distance from the shoulder was the same as the blunt nose configuration to within the resolution of the photographs. It had been determined in the earlier investigation (Reference 1) that this stand-off distance was independent of nose configuration. Within the time between two sparks (i.e. 100 μsec) this shock envelope changed to a large angled conical shock which again emanated from the tip and encompassed nearly the entire forebody forcing the aftershock further downstream. This remained the flow field until the end of the test. See figure 8.

This abrupt change in flow field was also reflected in the pressure traces. At one millisecond after the peak the mean pressure level as recorded by a Hidyne gauge at station 2 showed a drop to less than half its initial value and also an attenuation of the superimposed pressure fluctuations. Although the output of the BBN pressure sensors as recorded on the oscilloscopes are difficult to interpret, they are in agreement qualitatively with the Hidyne traces.

On re-examination of the previous tests of Reference 1, it was found that this phenomenon was present in every case, but overlooked due to the fact it took place between 15 and 23 msec after the peak, a time at which the temperature of the flow is so low that test gas condensation is considered to have occurred.This discontinuity is tentatively concluded to be a result of the reduction of Reynolds number during the test to such a value that the flow can no longer negotiate the pressure gradient produced by the isentropic compression. The result is that the extent of the separated region increases substantially. The high speed ciné schlieren substantiate this since as described earlier the foreshock angle is greatly enlarged after this supposed "critical" Reynolds number is reached. With this rapid increase in separated length the very efficient isentropic compression mechanism occurring early on the forebody surface is destroyed causing the drop in pressure. The relatively noise free-signal found after the pressure drop indicates that the flow in the separated region is steady.

Since this test and those of Reference 1 were not carried out at the same initial conditions and that condensation was present, it is not feasible at this point to calculate the values of these "critical" Reynolds numbers. However, there appears to be a trend that this Reynolds number decreases with increasing nose radius. See Figure 9. It should be noted that researches at Langley (Reference 16) observed similar but not identical trends at Mach 8.8 on tension shell shapes.

2. RESULTS OF EXPERIMENTS USING THE AEROTHERM ELLIPTICAL TRICONIC MODEL

a. Response characteristics of Kulite pressure transducers

It is seen in figure 10 two markedly different signal characteristics obtained from the Kulite transducers during

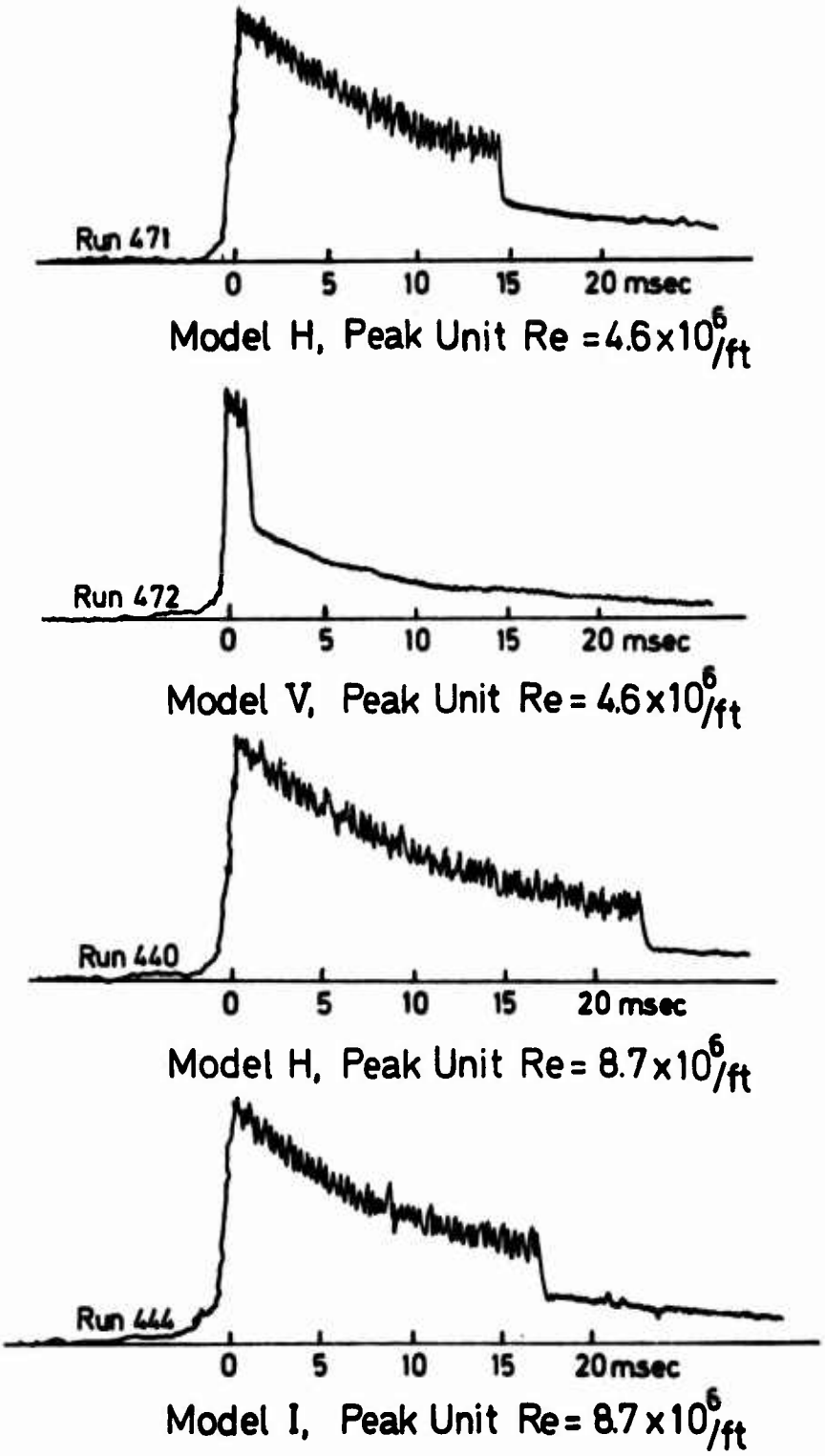

Figure 9. Effect of Nose Radius and Re on the Mean Pressure Level

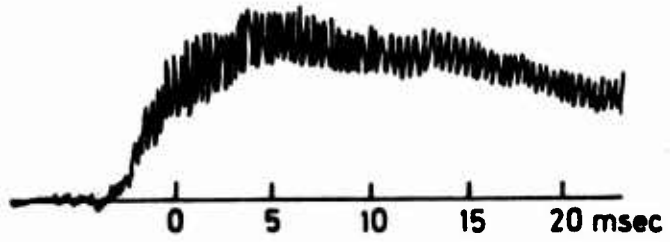

Stations 1 and 2 (Kulite)

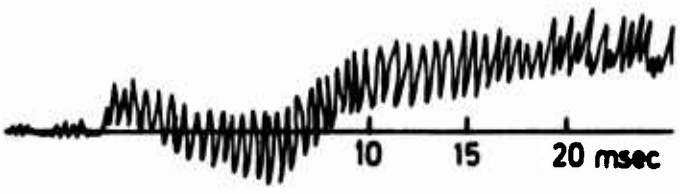

Stations 3 and 4 (Kulite)

Pitot Pressure (Hidyne)

Figure 10. Representative Output from Kulite Gauges

this phase of the investigation. A pitot pressure trace has been included in this figure to act as a time reference. Although four identical transducers were used, the results consistently yielded traces nearly identical to the upper sketch in Figure 10 at stations 1 and 2 and to the middle sketch at stations 3 and 4.

These signals can be considered as providing both mean and fluctuating pressure data. It is thus observed that the sample trace from stations 1 and 2 rises more slowly to a mean pressure level than does the pitot pressure despite the fact that the former system has an inherently better time response. However, once a maximum value of the mean pressure is reached, typically 5 msec after the pitot pressure peak, the d.c. component decays approximately the same as does the pitot trace characteristic of Longshot operation.

The recorded signal representing stations 3 and 4 exhibited a very different trend. The mean pressure level, which should represent an absolute pressure (in that the reference pressure is vacuum) is negative from just after the pitot peak until 4 msec into the run. The time that the signal remained negative varied depending on the run and station-position, but the shape was similar in all cases. The d.c. component then increased from zero until approximately 10 msec into the run and remained constant for more than 50 msec.

Between tests each gauge was calibrated dynamically as described in section III-4 to check that the measuring systems were functioning properly and each responded as expected of gauges with the given makers specifications. In a subsequent test series (Reference 17) these same Kulite pressure transducers were installed on a convex model. The output traces obtained were identical to those obtained from Hidyne gauges with somewhat better response. These observations indi-

cated that under normal test conditions the gauges were functioning correctly. It was noted also that the fluctuating signals recorded were quite similar to those obtained by Pallone (Reference 11).

The cause for the anomolous mean pressure levels was believed to be due to spurious signals caused by either accelerations due to steady or unsteady forces on the model or temperature effects due to exposure to the hot gas (2500°K) behind the aftershock. It is felt that these effects would be most pronounced at the rear stations due to their location and orientation in the flow. That is, the gauges at station 3 and 4 are located behind a normal or nearly normal shock virtually at all times and are hence at higher pressure levels and in a hotter environment than stations 1 and 2. According to the manufacturers specifications the Kulite gauges are an order of magnitude more sensitive to acceleration in the axial direction than in the transverse direction. Figure 5 illustrates that at stations 3 and 4 the gauges axes are nearly parallel to the flow direction. It is likely that the instability process observed as described in later sections would cause the largest effect in the freestream direction and hence, would interact more strongly with the gauges mounted at these positions.

A final factor to consider is the time to establish the flow in a separated region. The following two examples taken from the literature give a rough idea of the times expected. Holden in a study on separation (Reference 18) presents a simple correlation of the establishment time for the wake flow of spheres in hypersonic flow. This correlation and the equivalent parameters of this study yields a flow establishment time of 2.0 msec for the present test. According to Needham (reference 19) the flow establishment for a hypersonic laminar separated region in a compression corner is somewhat less than 1 msec.

Comparison of these flow establishment times with the time of the slow build up in mean pressures at stations 1 and 2 described earlier show that the latter effect may indeed be due to flow establishment, and that the times for these unsteady flows to settle down take considerable longer than steady separated flows.

b. Observations of flow instability using Kulite pressure Transducers

For reasons given in the preceding section and because the primary interest of the present study is unsteady phenomena, emphasis will be placed on the measured fluctuating component of the pressure traces in the following discussion.

Figure 11 presents the pressure traces obtained from run 470. These demonstrate clearly that the flow was unstable. From these traces and their counterparts from the other runs the following observations were made.

1. In the first 5 msec of run from the peak, the frequency of these fluctuations as recorded at stations 3 and 4 was 2.5 kHz ($\pm$ 5 %). This frequency was apparently independent of nose roughness or geometry. The approximate Strouhal number based on model diameter is approximately 0.17.

2. In the tests in which the pulsation mode was observed there existed a distribution of $\Delta p/p_{t2}$ which could be considered relatively unaffected by model geometry or flow conditions. The values of $\Delta p/p_{t2}$ averaged over all tests were approximately 0.09, 0.18, 0.36, and 0.40 for stations 1 to 4 respectively. Although these values are somewhat lower than those obtained by Pallone (reference 11), they appeared to follow the same trend of decreasing $\Delta p/p_{t2}$ with increasing Reynolds number.

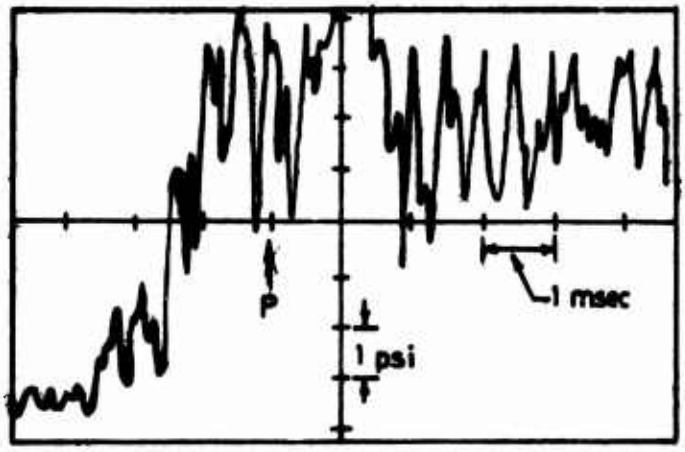

Station 1

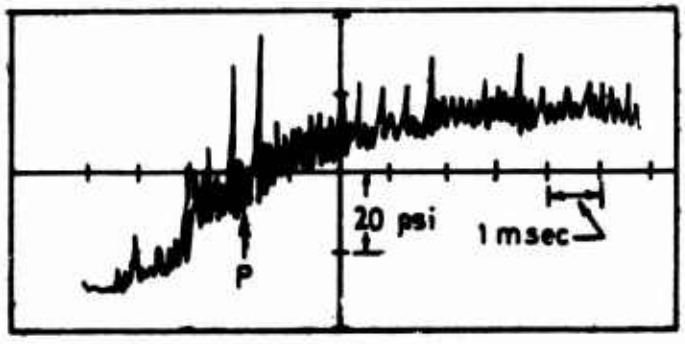

Station 2

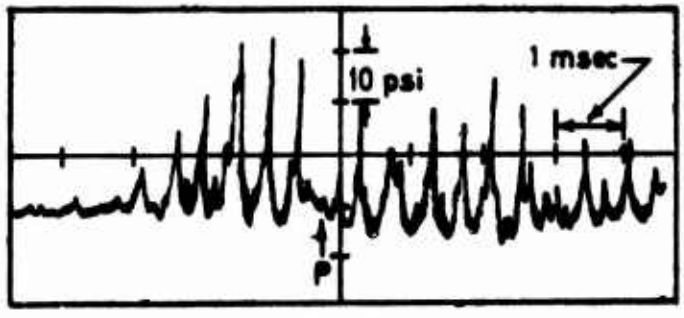

Station 3

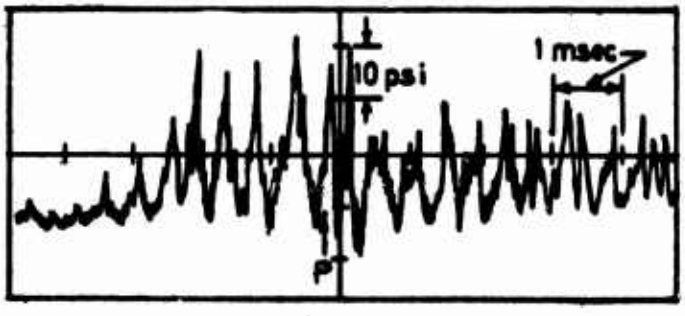

Station 4

Figure 11. Pressure Signals from Run 470

3. The characteristic wave-form of the fluctuation is more easily seen at stations 3 and 4 than at stations 1 and 2 (see Figure 11, on this figure the time at which peak freestream conditions occur is denoted by the letter "P"). At the earlier stations there was little similarity between consecutive pulses or sequences of pulses. Furthermore many of the larger pulses appear to contain a number of intermediate frequencies (between 4.5 and 7 kHz) probably due to the dynamic impulsive nature of the growth behaviour of the foreshock. For these reasons it is difficult to determine the dominating frequency of the instability from traces obtained at the earlier stations.

4. There appeared to be some correlation between the pressure histories of stations 3 and 4. However, there was some attenuation and phase shift occurring along the model which indicated large and changing pressure gradients on the body surface. This illustrates that it will be difficult to obtain any information from synchronisation of pressure traces and photographs of shock envelopes.

5. It was observed from the traces recorded on the oscillograph that the frequency of the instability decreased approximately 20 % after 20 msec from peak conditions. This is expected since for a constant Strouhal number the frequency will decrease with decreasing velocity as occurs with increasing time during a test in Longshot.

6. Both the oscillation and pulsation modes of instability were identified in the test at the high Reynolds number, 8.7×10^6/ft Mach 15 flow over the model fitted with the long rough nose (Run 467). Figure 12 presents the pressure signals obtained from this test. It is seen that the signal from station 2 exhibits two local maxima in the mean pressure level. The first maximum is approximately 2 msec after the peak pitot pressure and the second 4 msec later. After each peak the mean level decays as expected. The regions in which the mean pressure level rises coincides with

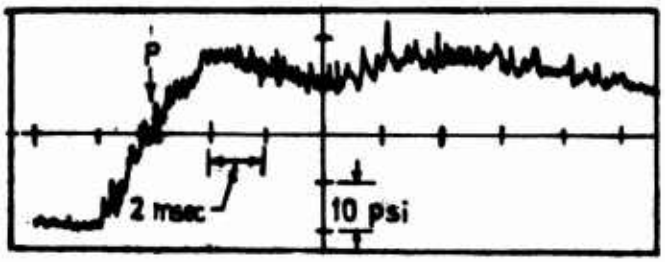

Station 2

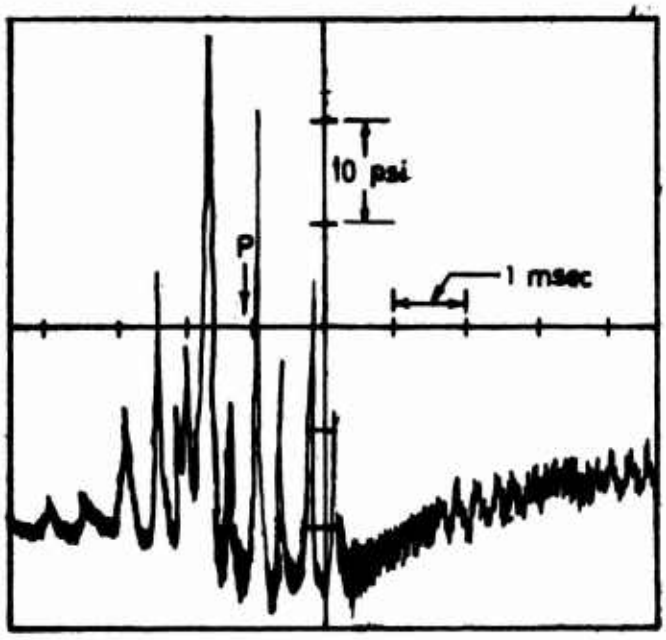

Station 3

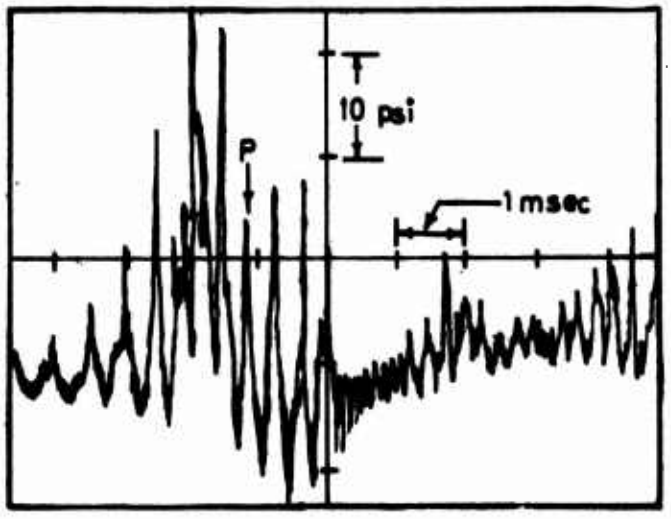

Station 4

Figure 12. Pressure Signals from Run 467

a change in the mode of instability, as seen in the high speed schlieren pictures described later, from oscillation to pulsation, oscillation occurring in the time between 2 and 6 msec after the peak.

Although at present there exists inadequate detailed knowledge of the flow field over such concave bodies, this change in the mean pressure level could be explained in two possible ways assuming the flow charges oscillation to pulsation modes of instability. First, in the oscillation mode the foreshock away from the nose is always an oblique shock with an aftershock generated by compression waves originating from the shoulder region. The mean pressure associated with this shock envelope would be less than that generated by the pulsation shock envelope with its strong normal shock which at times is the only shock in evidence in the forebody region. A second approach lies in considering the isentropic compression afforded by the concave forebody as seen on some concave models (see Reference 1). Because the oscillation mode of instability is always accompanied by a substantial separated region (see Figure 3) the mechanism of isentropic compression is expected to be suppressed at all times. Isentropic compression however, may occur for the pulsation mode during part of the cycle. Hence a higher mean pressure than that of a process involving a separated region such as the oscillatory mode would be expected. A combination of these two possibilities with each one dominating a different part of the cycle is likely to exist.

The remaining two traces on the oscillograph show that between 2 and 6 msec after the peak the amplitude of the fluctuating pressure given by Δp is approximately 20 % of that at other times. These observations concerning the mean and fluctuating behaviour of the traces indicate the presence of the ocillatory mode of instability during the period from 2 msec to 6 msec after the peak. Summarising, the oscillation mode would be expected to have a somewhat higher frequency and smaller amplitude since the change in the shock envelope is small compared to the pulsation mode.

7. The oscillation mode of instability occurred only during the test on the model fitted with the long rough tip at high Reynolds number i.e. conditions that produced the highest possibility of boundary layer transition. Similar to results found on the Concave Biconic model this suggests again that there exists a "critical" Reynolds number above which, in this case, the flow is of the oscillation mode and below which it is of the pulsation mode of instability. The hypothesis of a critical Reynolds number is further born out since this same model, when tested at a lower critical Reynolds number, exhibited only the pulsation mode.

Referring again to figure 12, it is seen that there was pulsation during the first 1 or 2 msec of run. This was attributed to transients remaining after the flow passed through lower Reynolds number conditions in the build up to peak conditions early in the test.

c. Results from the high speed ciné schlieren

The high speed ciné schlieren films from runs 460 to 470, presented in figures 13 through 16, illustrate clearly an unstable flow field over the Elliptical Triconic model. In each figure, the frame coinciding with the peak condition is marked with a letter P.

The predominant form of instability seen in these figures is the pulsation mode using the spiked blunt body terminology given in the Introduction. It is seen to be a regular process. For example, in Figure 14 the first frame after the peak conditions of Run 468 illustrates that a nearly conical shock created by the nose exists. In the next two frames this conical shock expands to a spherical shape until the aftershock originating from the blunt afterbody of the model is displaced. By the following frame (i.e. 100 μsec later) this bubble-like shock has collapsed leaving what appears to be some highly mixed

flow on the forebody and a very weak conical shock emanating from the tip. The process then repeats itself.

In Figures 17 and 18 plots of the "volume" of the conical foreshock versus time are given. The quantity plotted along the ordinate to illustrate the volume is the diameter of this shock measured at right angles to the model axis at an arbitrary distance from the tip. Even though these plots are built up from information measured at discrete times they yield frequencies with approximately the same values as those obtained from the pressure signals (see section IV2b).

Of special interest is the period between 2 and 6 msec after the peak in run 467 (Figure 17). This agrees well with findings from pressure traces of this run discussed in the previous section. During this period the foreshock is a relatively large angle conical shock which oscillates between slightly concave and slightly convex dispositions. Its frequency is difficult to determine since its apparent value is a large fraction of the framing rate (i.e. 4-5 kHz compared to 10,000 frames per sec). This frequency as well as the others are also in agreement with those obtained from the pressure traces.

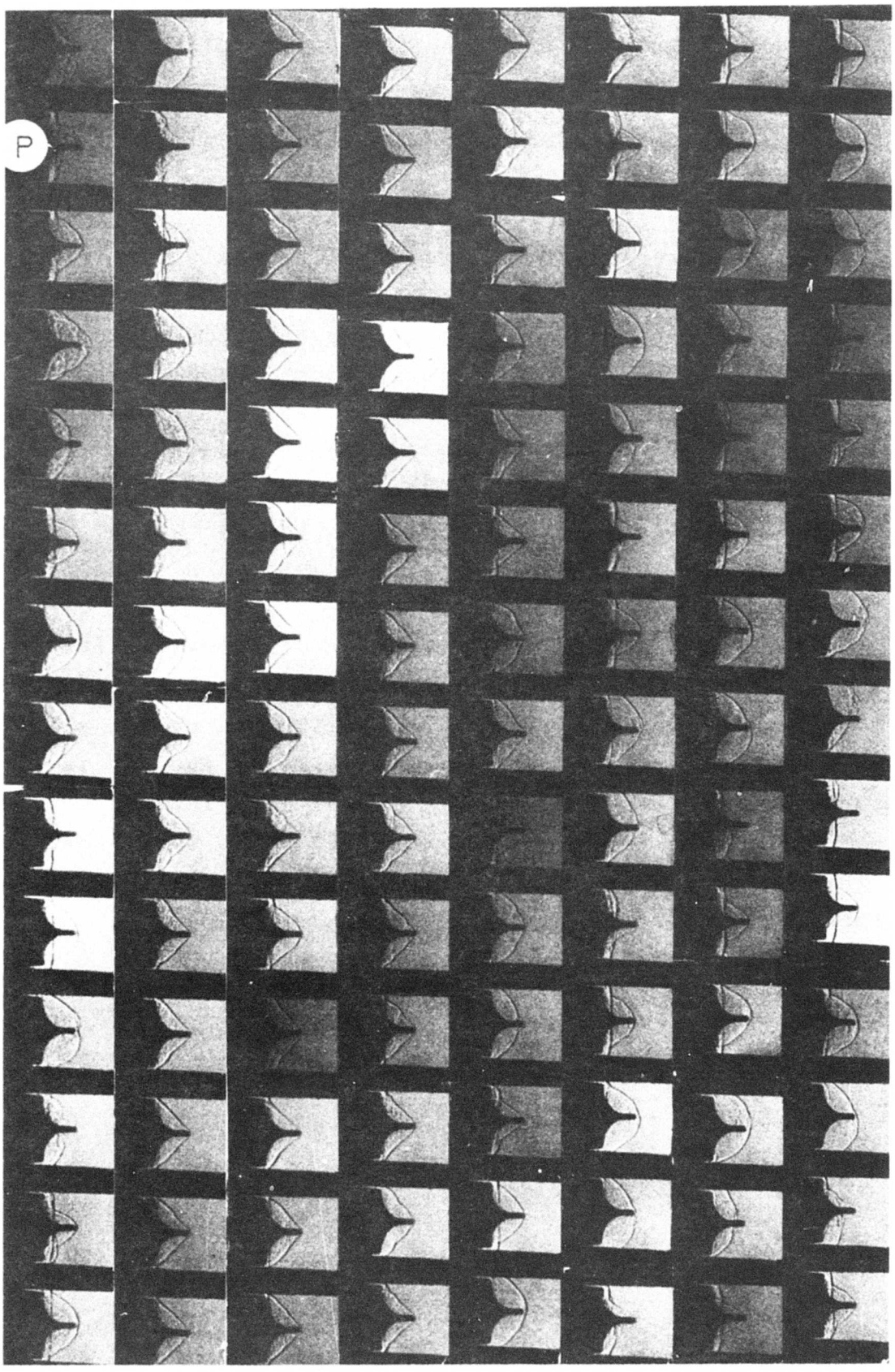

Figure 13. Run 467 High Speed Ciné Film

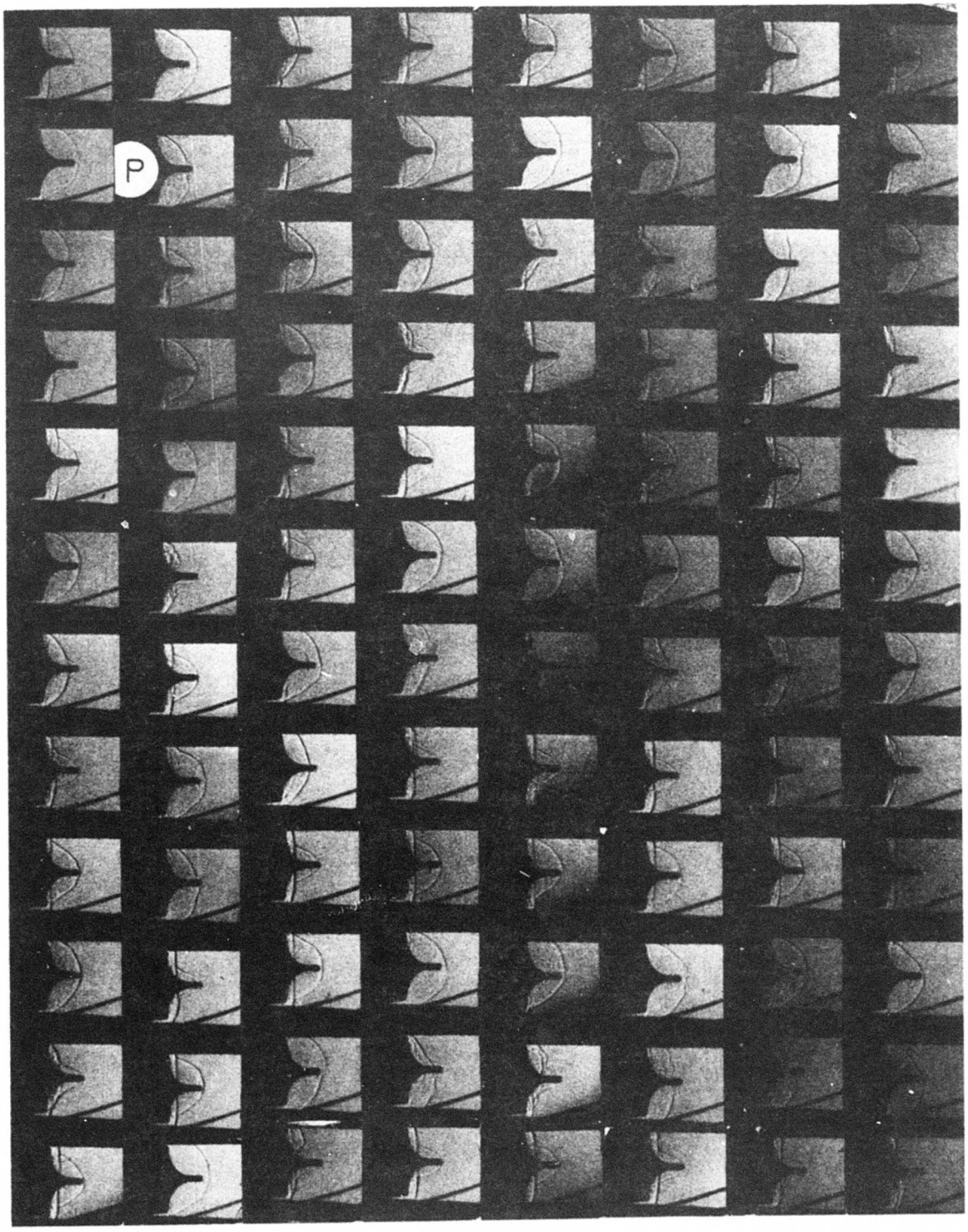

Figure 14. Run 468 High Speed Ciné Film

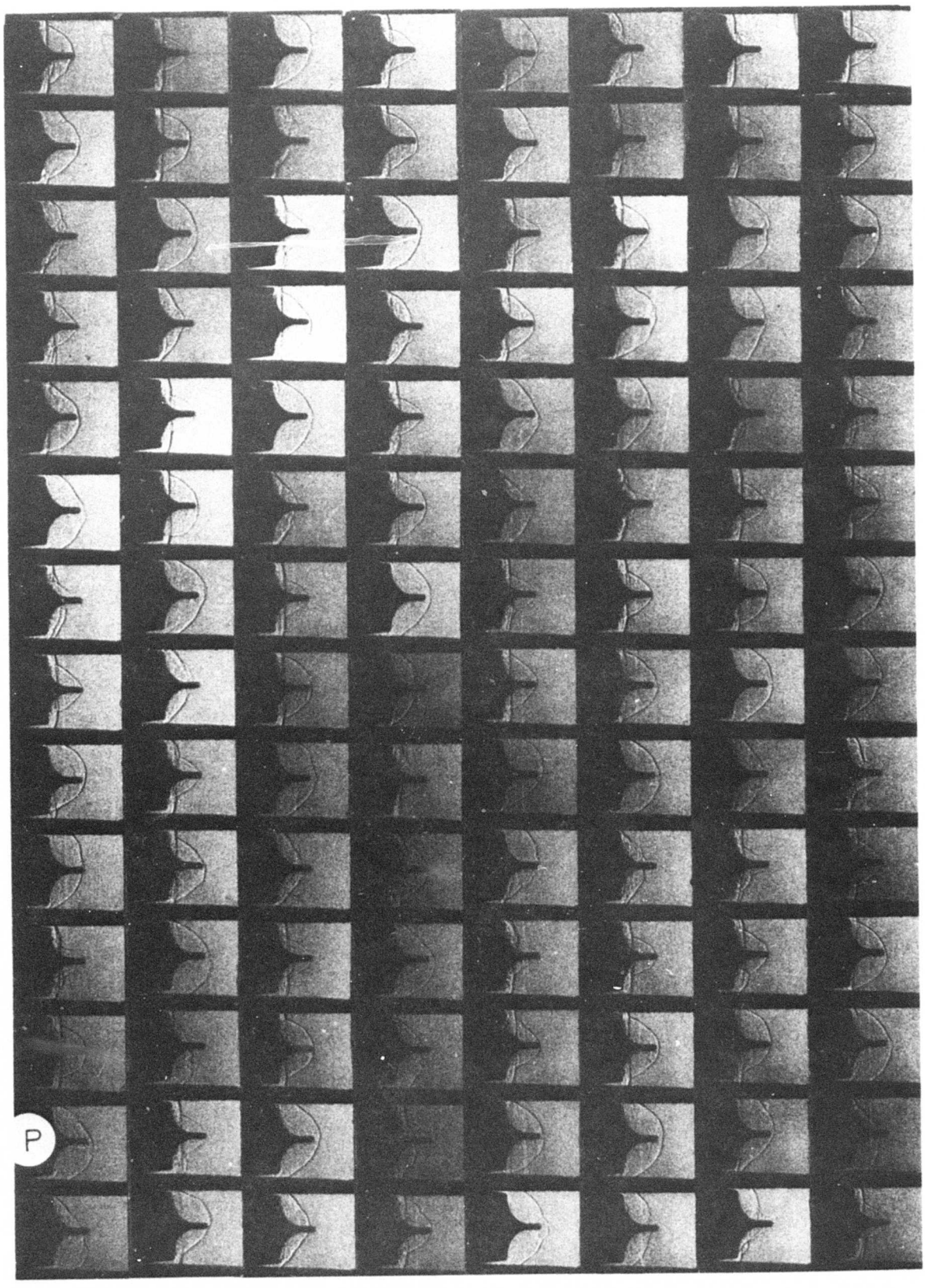

Figure 15. Run 469 High Speed Ciné Film

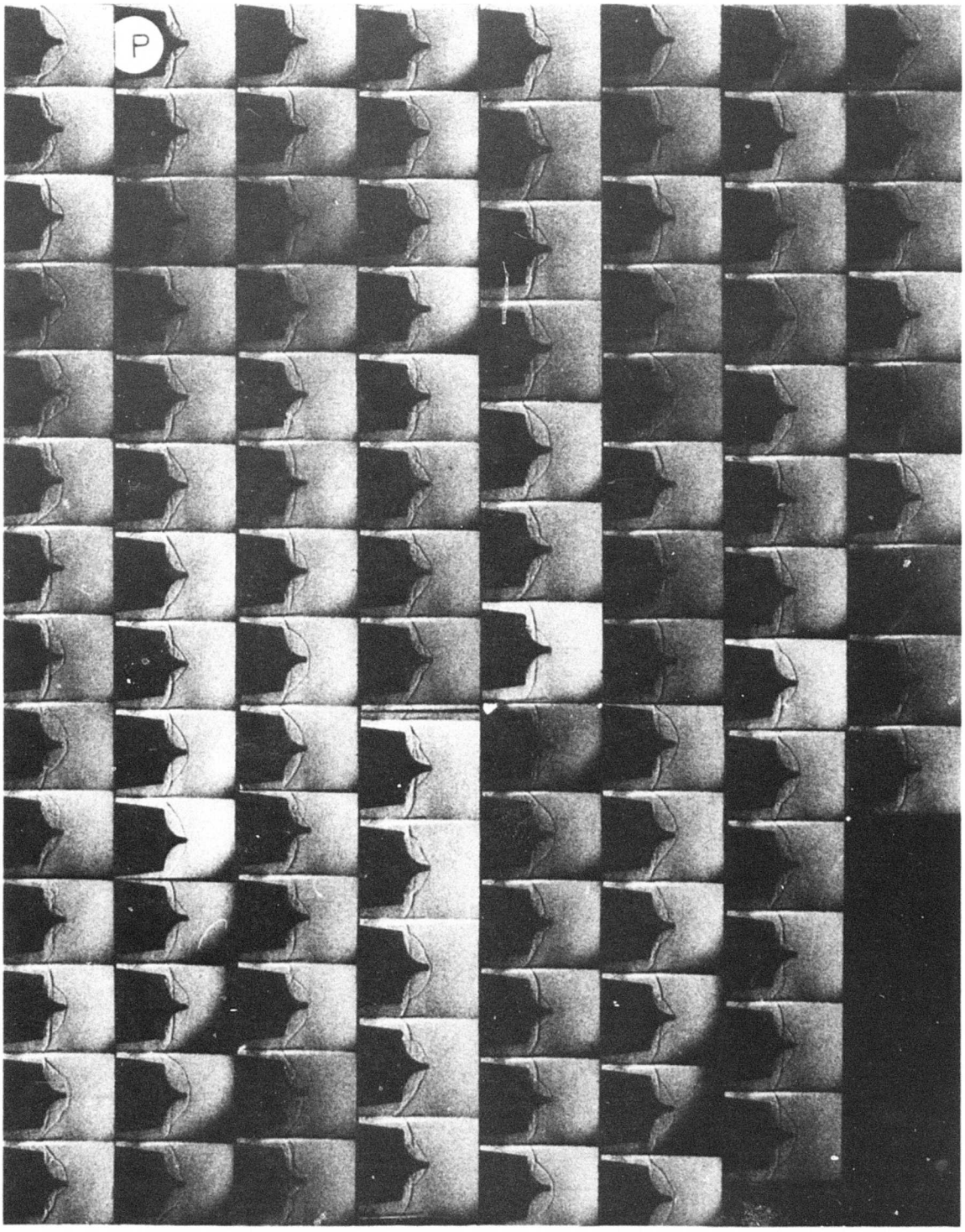

Figure 16. Run 470 High Speed Ciné Film

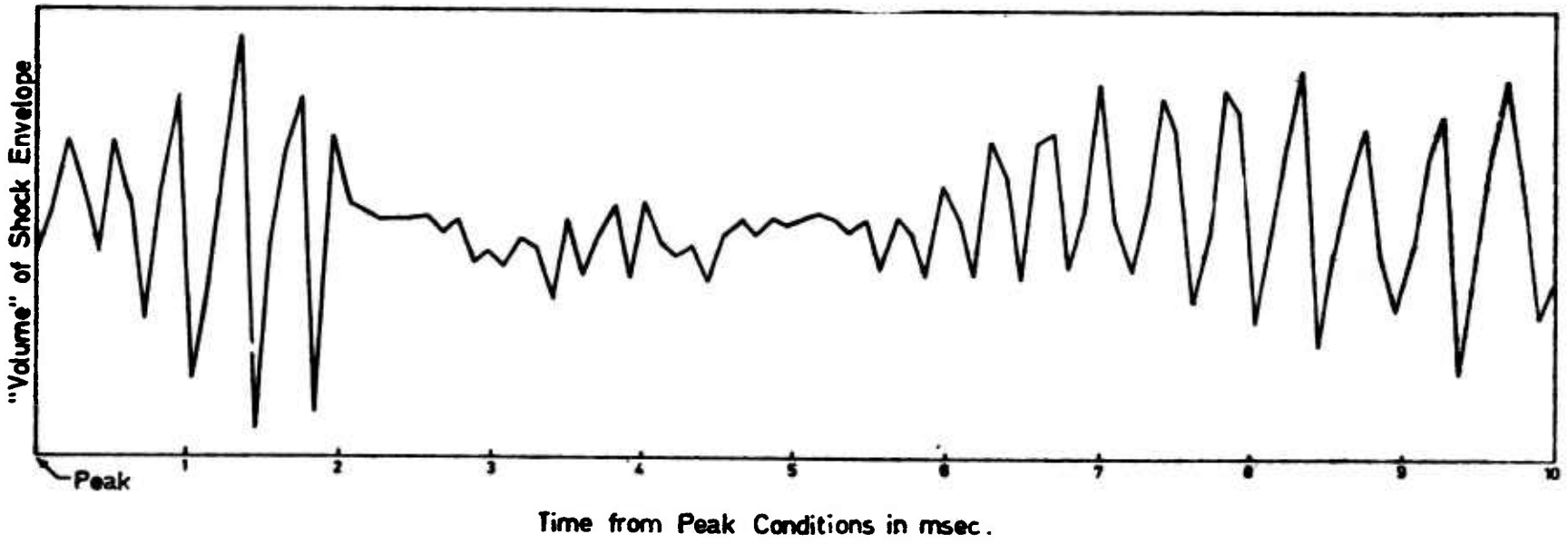

Figure 17. "Volume" of Shock Envelope vs. Time for Run 467

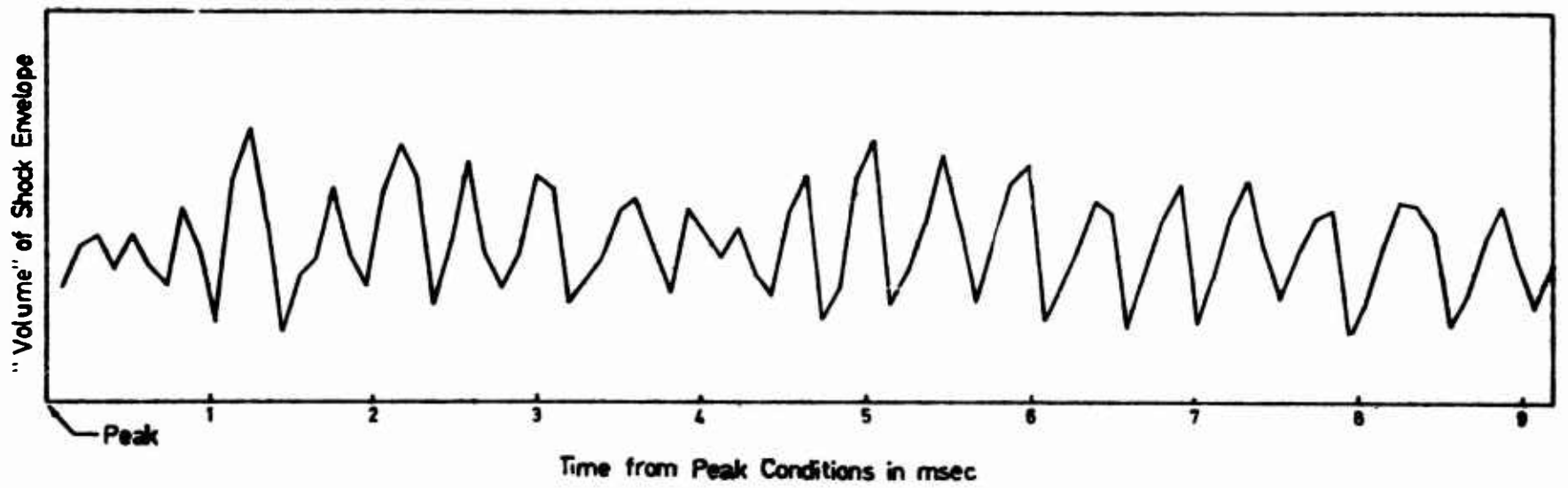

Figure 18. "Volume" of Shock Envelope vs. Time for Run 470

SECTION V

CONCLUSIONS

A study of the unsteady flow over concave conic shapes has been made using a high speed ciné photograph technique and fast response instrumentation in the flow in the VKI Longshot windtunnel, simulating the high Reynolds number high Mach number phase of re-entry flight. The results have hinted that other than the pulsation mode of instability, two other modes of instability flow associated with spiked blunt bodies were present under certain conditions.

A regular 7 kHz (equivalent to $fD/u = 0.4$) pressure signal sensed on the Concave Biconic model at a high Reynolds number condition was ascribed to the pressure of the "vibrational" instability mode. The expected shock movement was too small to be seen in the photographs. At lower Reynolds numbers large, but fairly stable separate regions were found to be present.

The oscillation mode was observed on the Elliptic Triconic model at such conditions that transitional or turbulent flow was most likely to have occured on the concave surface. The frequency of the fluctuation was approximately 4 to 5 kHz i.e. $fD/u = 0.27$ to 0.33. At all other conditions the pulsation mode was found to exist occurring always at a frequency of approximately 2.5 kHz (i.e. $fD/u = 0.17$). The amplitudes of pressure fluctuations sensed on the concave surface in the "pulsation" unstable mode had the highest values seen during the test which varied from $0.09\ p_{t2}$ near the nose to $0.40\ p_{t2}$ near the shoulder.

The above conclusions are considered somewhat tentative in the light of the present know-how about these flow instabilities. It is recommended that a well-planned study be carried out to understand the flow process involved in the instability over spiked cones and their derivatives and to define further the boundaries within which they exist.

REFERENCES

1) B.E. Richards, and M.A. Kenworthy, "Steady Hypersonic Flow over Axisymmetric Concave Conic Shapes" Interim Scientific Report, Grant AFOSR-72-2227, Jan. 1974. AFML-TR-75-137.

2) H.J. Allen, and A.J. Eggers, Jr., "A Study of the Motion and Aerodynamic Heating of Missiles entering the Earth's Atmosphere at High Supersonic Speeds." NACA TN 4047, 1957.

3) W.F. Moeckel, "Flow Separation ahead of Blunt Bodies at Supersonic Speeds." NACA TN 2418, 1951.

4) W.A. Mair, "Experiments on Separation of Boundary Layers on Probes in front of Blunt Nosed Bodies in a Supersonic Air Stream." The Phil. Mag., July 1952.

5) D. Beastall, and J. Turner, "The Effect of a Spike Protruding in front of a Bluff Body at Supersonic Speeds." ARC, R & M No 3007, 1957.

6) S.M. Bogdonoff, and I.E. Vas, "Preliminary Investigations of Spiked Bodies at Hypersonic Speeds." Princeton U. Report No 412, 1958.

7) D.J. Maull, "Hypersonic Flow over Axially Symmetric Spiked Bodies." JFM Vol. 8, 1960.

8) C.J. Wood, "Hypersonic Flow over Spiked Cones." JFM Vol. 12 Pt. 4, 1961.

9) M.S. Holden, "Experimental Studies of Separated Flows at Hypersonic Speeds." Part I : Separated Flows over Axisymmetric Bodies. AIAA J., Vol. 4, 1966, pp. 591-599.

10) H.P. Kabelitz, "Zur Stabilität geschlossener Grenzschicht-ablösegebiete an konischen Drehkörpern bei Hyperschall-anströmung." DLR FB 71-77, 1971.

11) A. Pallone (private communication), 1973.

12) B.E. Richards, and K.R. Enkenhus, "Hypersonic Testing in VKI Longshot Piston Tunnel." AIAA Journal, Vol. 8, No 6, June 1970.

13) B.E. Richards, S. Culotta, and J. Slechten, "Heat Transfer and Pressure on Re-entry Nose Shapes in the VKI Longshot Hypersonic Tunnel." AFML-TR-71-200, Wright Patterson AFB, Ohio, June 1971.

14) H.H. Heller, and A.R. Clemente, "Unsteady Aerodynamic Loads on Slender Cone/Flat Base Configurations at Free-stream Mach Numbers from 0 to 22." AIAA Paper 73-998, presented at AIAA Aero Acoustic Specialist Conference, Seattle, U.S.A., Oct. 1973.

15) R.J. Pallant, "A Note on the Design and Construction of a Low Pressure Calibrator and a Comparison with Shock Tube and Static Calibration Methods." British A.R.C. CP 947, 1966.

16) R.A. Jones, D.M. Bushnell, and J.L. Hunt, "Experimental Flow Field and Heat Transfer Investigation of Several Tension Shell Configuration at a Mach Number of 8." NASA TN-D-3800, Jan. 1967.

17) B.E. Richards, and M.A. Kenworthy, "Pressure Measurements on a Convex Biconic Model in a Mach 15 Flow." Test Report 84, Grant AFOSR 72-2227, March 1974.

18) M.S. Holden, "Experimental Studies of Shock Wave - Boundary Layer Interaction", VKI Short Course, Lecture Series 62, Jan. 1974.

19) D.A. Needham, "Laminar Separation in Hypersonic Flow" Ph.D. Thesis submitted to the University of London, Aug. 1965.

☆ U.S. GOVERNMENT PRINTING OFFICE: 1976 — 657-630/316